Contour Tracking of Images Using Particle Filtering Technique.

Sreedevi M T [1], Shobha B S [2]

[1]Department of Electronics & Communication Engineering, D A C G Government Polytechnic Chikkamagaluru-577101

[2]Department of Mechanical Engineering, D A C G Government Polytechnic Chikkamagaluru-577101

Abstract

A Monte Carlo algorithm for extracting contours in 2D images is proposed in this paper. A multiple model Particle Filter (PF) for progressive contour growing (tracking) from a starting point is designed, accounting for the convex, noncircular form of delineated areas. The algorithm relies on image intensity gradients as measurements and requires information about four manually selected points: the seed point, the starting point, arbitrarily selected on the contour, and two additional points, bounding the measurement formation area around the contour. The filter performance is studied by segmenting contours from series of simulated ultrasound medical images and Ground Penetrating Radar (GPR) images.

1. Introduction

The problem of automated or semi-automated contour following can be considered from a probabilistic point of view: the contours are realizations of a stochastic process driven by both an inner stochastic dynamics, and a statistic data model [1]. The Bayesian methods for tracking provide a probabilistically consistent way for combining prior information with data to produce efficient solutions. A number of tracking techniques are proposed for contour extraction and successfully applied to medical images, such as Kalman filtering, multiple hypothesis tracking, combined interacting multiple model (IMM) estimation and probabilistic data association filtering (PDAF) [2].

A robust particle filtering algorithm for contour following is developed in [1]. The potential of this algorithm (called Jetstream) is demonstrated in the context of the interactive cut-out in photo- editing applications. Jetstream is a general tool for designing contour tracking algorithms in different application areas. The designer has the freedom to choose appropriate task oriented ingredients: dynamics and measurement models, likelihoods or likelihood ratios and constraints.

This paper investigates further the capabilities of Jetstream for the purposes of segmentation in ultrasound medical and GPR images. The new elements of the proposed algorithm, compared with Jetstream [1], include: 1. implementation of a multiple model structure of the prior dynamics, governing the predicted contour growing; 2. combined likelihood based on the intensity gradient and second order directional derivatives; 3. incorporation of constraints accounting for the convexity of the contour.

2. Contour Tracking by Particle Filtering

Consider a state vector $\mathbf{x}$, containing points $\mathbf{x}_k$ in the image plane $\mathbf{\Lambda} \subset \mathbf{R}^2$. Any ordered sequence $\mathbf{x}_{0:n} = (\mathbf{x}_0, \ldots, \mathbf{x}_k, \ldots, \mathbf{x}_n) \in \mathbf{\Lambda}^{n+1}$ uniquely defines the contour being tracked [1]. Given the prior state probability density function $p(\mathbf{x}_{k+1} | \mathbf{x}_{0:k})$, modeling the expected evolution of the contour, the aim is to enlarge the sequence, using the measurement data model $p(\mathbf{y} | \mathbf{x}_{0:n})$. Often the measurement $\mathbf{y}(\mathbf{x}_k)$ is the gradient norm of image intensity $|\nabla \mathbf{I}(\mathbf{x}_k)|$.

Assuming a first-order dynamics $p(\mathbf{x}_{k+1} | \mathbf{x}_{0:k}) = p(\mathbf{x}_{k+1} | \mathbf{x}_k)$, $k \geq 1$, a prior state density on $\mathbf{\Lambda}^{n+1}$ is given by $p(\mathbf{x}_{0:n}) = p(\mathbf{x}_0) \prod_{k=1}^{n} p(\mathbf{x}_k | \mathbf{x}_{k-1})$. The measurement data conditioned on $\mathbf{x}_{0:n}$, are approximated by an independent spatial process $p(\mathbf{y} | \mathbf{x}_{0:n}) \square \square_{u\square\square} p(\mathbf{y}(u) | \mathbf{x}_{0:n})$, where $\square \square \mathbf{\Lambda}$ is a discrete set of measurement locations in the image plane, including the $\mathbf{x}_k$ locations. Each term (likelihood) in the product is p_{on} if the pixel u belongs to $\mathbf{x}_{0:n}$, or p_{off} if u is out of the contour [1]:

$$p(\mathbf{y} | \mathbf{x}_{0:n}) \square \square_{u\square\square\backslash\mathbf{x}_{0:n}} p_{off}(\mathbf{y}(u)) \square_{k\square 0}^{n} p_{on}(\mathbf{y}((\mathbf{x}_k) | \mathbf{x}_{0:n}) \square \square_{u\square\square} p_{off}(\mathbf{y}(u)) \square_{k\square 0}^{n} \frac{p_{on}(\mathbf{y}((\mathbf{x}_k) | \mathbf{x}_{0:n})}{p_{off}(\mathbf{y}((\mathbf{x}_k))}$$

Up to a multiplicative factor independent from represented by $\mathbf{x}_{0:n}$, the posterior state density on $\mathbf{\Lambda}^{n\square 1}$ is

$$p_n(\mathbf{x}_{0:n} | \mathbf{y}) \square p(\mathbf{x}_0) \square^{n}_{k=1} p(\mathbf{x}_k | \mathbf{x}_{k\square 1}) \prod_{k\square 0}^{n} \ell(\mathbf{y}(\mathbf{x}_k)), \quad (1)$$

where $\ell \square p_{on} / p_{off}$ denotes the point-wise likelihood ratio. If the starting point is picked by the user, the density $p(\mathbf{x}_0)$ is a Dirac mass centered at this location. The contour extraction problem, expressed as the minimisation of the function $\square_n(\mathbf{x}_{0:n}, \mathbf{y}) \square \square \log p_n(\mathbf{x}_{0:n} | \mathbf{y})$ can be solved by finding the maximum a posteriori (MAP) estimate of the posterior state probability density function (pdf). Following the Bayesian methodology, the state pdf (1) can be recursively calculated according to the relationship

$$p_{k\square 1}(\mathbf{x}_{0:k\square 1} | \mathbf{y}) \square \ell(\mathbf{y}(\mathbf{x}_{k\square 1})) \, p(\mathbf{x}_{k\square 1} | \mathbf{x}_k) \, p_k(\mathbf{x}_{0:k} | \mathbf{y})$$

.

(2) Analytical solution to (1) is intractable. Within the sequential Monte Carlo framework, the posterior density $p_k(\mathbf{x}_{0:k} | \mathbf{y})$ is approximated by a finite set $\{\mathbf{x}^{(j)}_{0:k}\}, j \square 1,\ldots,N$ of N sample paths (particles). The generation of samples from $p_{k\square 1}(\mathbf{x}_{0:k\square 1} | \mathbf{y})$ is obtained in two steps of prediction and update, thoroughly explained in the specialised literature [3]. At the prediction (importance sampling) step, each path $\mathbf{x}^{(j)}_{0:k}$ is grown of one step $\tilde{\mathbf{x}}^{(j)}_{k\square 1}$ by sampling from the proposal density function $q(\mathbf{x}_{k\square 1} | \mathbf{x}^{(j)}_{0:k}) \square p(\mathbf{x}_{k\square 1} | \mathbf{x}^{(j)}_k)$. At the update step, each sample path (contour) is associated with a weight, proportional to the likelihood ratio of the measurements $w^{(j)}_{k\square 1} \square w^{(j)}_k \ell(\mathbf{y}(\tilde{\mathbf{x}}^{(j)}_{k\square 1}))$. The set of weighted paths $\{\tilde{\mathbf{x}}^{(j)}_{0:k+1}, \tilde{w}^{(j)}_{k+1}\}, j \square 1,\ldots,N$ with normalised weights $\tilde{w}^{(j)}_{k+1} \square w^{(j)}_{k+1} / \sum_{j=1}^{N} w^{(j)}_{k+1}$ provides an approximation to the distribution $p_{k\square 1}(\mathbf{x}_{0:k\square 1} | \mathbf{y})$. When an estimate of the effective sample size $N_{eff} = 1 / \sum_{j\square 1}^{N} (\tilde{w}^{(j)}_k)^2$ falls below a threshold N_{thresh}, resampling is realised to avoid possible degeneracy of the sequential importance sampling [3]. Based on the discrete approximation of the posterior pdf $p_{k\square 1}(\mathbf{x}_{0:k\square 1} | \mathbf{y})$, an estimate of the 'best' path (contour) at step $k \square 1$ can be obtained. The path of a maximum weight (before resampling) provides an approximation of the MAP estimate. The mean $E(\mathbf{x}_{0:k\square 1} | \mathbf{y}) \square \square_{j\square 1}^{N} w^{(j)}_{k\square 1} \tilde{\mathbf{x}}^{(j)}_{0:k\square 1}$ is a Monte Carlo approximation of the posterior pdf expectation.

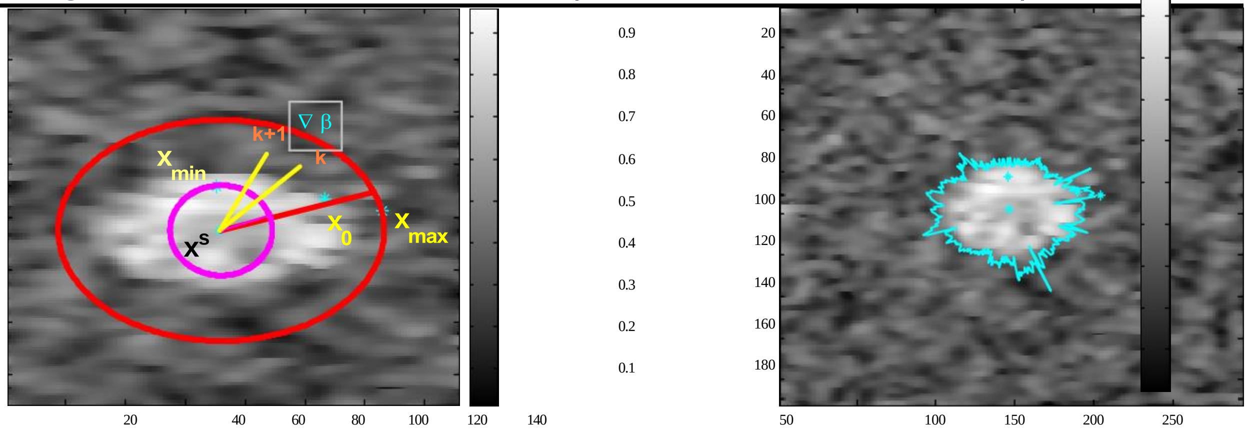

Fig.1. a) The sampling angle between radii k and $k+1$. The points $\mathbf{x}_s$, $\mathbf{x}_0$, $\mathbf{x}_{min}$, $\mathbf{x}_{max}$ are manually selected by the mouse. b) The result of ultrasound lesion segmentation.

Let $\mathbf{x}^s = (x^s, y^s)^T$ be the location of the seed point in the Cartesian coordinate frame, centered at the left and low corner of the image (Fig.1.a). Let $\mathbf{d} = (d, \theta)^T$ be the location of an arbitrary image point in the relative polar coordinate system, centered at the seed point. Consider the following model of a discrete-angle jump Markov contour dynamics

$$\mathbf{d}_{k+1} = \mathbf{F}\,\mathbf{d}_k + \mathbf{G}\,\mathbf{u}_{k+1}(m_{k+1}) + \mathbf{B}\,v_{k+1}(m_{k+1}), \quad (3)$$

where $\mathbf{d}_k = (d_k, \theta_k)^T$ is the base (continuous) state vector, representing contour point coordinates along the radius k, $\mathbf{F}$ is the state transition matrix and $\mathbf{u}_k$ is a known control input. The process noise $v_k(m_k)$ is a white Gaussian sequence with known variance $v_k \sim N(0, \sigma_d^2(m_k))$. The modal (discrete) state $m_k \in S = \{1, 2, \ldots, s\}$, characterising the different system models, is evolving according to a Markov chain with known transition probabilities $\pi_{ij} = \Pr\{m_{k+1} = j \mid m_k = i\}, (i, j \in S)$ and initial probability distribution $P_0(i) = \Pr\{m_0 = i\}$.

Denote the sampling angle between the subsequent radii as $\Delta\theta$. The control input of the form $\mathbf{u}_{k+1}(m_{k+1}) = (\Delta d_{k+1}(m_{k+1}), \Delta\theta)^T$ governs the changes in the state. Suppose that the mode set S contains $s = 3$ elements. Each model in the set corresponds to a fixed, predetermined distance increment $\Delta d_{k+1}(m_{k+1})$: $\Delta d_{k+1} = 0\ (m = 1)$ models the "move" regime along the circle, since the distance d_k does not change. The increments Δd_{k+1} (for $m = 2, 3$) are constants corresponding to the distance increase or decrease, respectively. The process noise v_k models perturbations in Δd_{k+1}. The matrices $\mathbf{F}, \mathbf{G}, \mathbf{B}$ have a simple form: $\mathbf{F} = \mathbf{G} = (1\ 0; 0\ 1)$, $\mathbf{B} = (1\ 0)'$. In the framework of this model, the state vector $\mathbf{x}_k = (x_k, y_k, d_k, \theta_k)^T$ contains both the Cartesian coordinates of contour point according to the left-down image corner and the polar coordinates, according to the internal seed point.

Constraints. Taking into account the proposed convex form of the contour, the area of measurement formation is bounded by an inner circle and an outer ellipse (Fig.1.a). Two points, $\mathbf{x}_{min}$ and $\mathbf{x}_{max}$, chosen by the mouse, determine the gating area. The distances d_{max} and d_{min} of the points in the polar coordinate system correspond to the major semi-axis of the ellipse Re_{max} and the circle radius R_c respectively. The variable $\Delta = Re_{max} - R_c$ is a design parameter. The minor semi-axis of the ellipse is calculated according to the relationship $Re_{min} = R_c + 2/3 Re_{max}$.

Suppose that a cloud of N particles $\tilde{\mathbf{x}}^{(j)}_{0:k+1}$, $j = 1, \ldots, N$ is predicted at the angle step $k+1$, according to the state evolution equation (3). At this stage, constraints are imposed in such a way, that particles outside the boundaries, accept the coordinates of the boundaries. Then, a likelihood ratio is computed for each particle point, situated inside the boundaries.

Likelihood ratio ℓ. The gradient norm of image intensity $|\nabla \mathbf{I}(\mathbf{x}_k)|$ is a principal likelihood component. According to the definitions introduced in Sec. 2, we have explored the gradient norm distribution both off contours (p_{off}) and on contours (p_{on}) over a series of images. The empirical distribution of the gradient norm off contours (on the whole image data) confirmed the results, obtained in [1]. The gradient norm distribution can be approximated by an exponential distribution with a parameter μ , which is the average gradient norm.

However, the empirical distribution of the joint gradient norm and gradient direction on the contour p_{on}, obtained and implemented in [1], is not satisfactory in our application. For the purposes of GPR image segmentation, we found that the square root of gradient norm is a suitable p_{on} measure. In regard to the medical images, we adopt an approach of combining the gradient norm and an edge detection algorithm, proposed in [2]. The aim is to utilise gradient information simultaneously along the $x \times y$ axes and along the radii, projected from the seed point, in order to improve the edge detection sensitivity.

Note that N predicted particles $\tilde{\mathbf{x}}^{(j)}_{0:k+1}$, $j = 1,\ldots,N$ are located along the radius, determined by the angle θ_{k+1} in the relative polar coordinate system. Let N_c candidate edge points $\mathbf{r}_i = (d_i, \theta_{k+1})^T$, $i = 1,\ldots,N_c$, satisfying the imposed constraints, are selected on the segment. The edge magnitude of each point $\mathbf{r}_i$ is calculated according to [2]

$$F_{edge}(d_i, \theta_{k+1}) = 1/3\{\mathbf{I}(d_i + 2\Delta r, \theta_{k+1}) + \mathbf{I}(d_i + \Delta r, \theta_{k+1}) + \mathbf{I}(d_i, \theta_{k+1}) - \mathbf{I}(d_i - \Delta r, \theta_{k+1}) - \mathbf{I}(d_i - 2\Delta r, \theta_{k+1}) - \mathbf{I}(d_i - 3\Delta r, \theta_{k+1})\}(1 - \mathbf{I}(d_i, \theta_{k+1}))^2,$$

where Δr is a differential radial increment from d_i along the radius (design parameter) and $\mathbf{I}(\mathbf{r}_i)$ is the local gray-level image intensity. The edge point with a maximum magnitude $\mathbf{r}_m = \max\{F_{edge}(\mathbf{r}_i), i = 1,\ldots,N_c\}$ takes part in the likelihood ratio computation. We propose two different likelihoods p^{US}_{on} and p^{GPR}_{on} for ultrasound and GPR images, respectively

$$p^{US}_{on}(\tilde{\mathbf{x}}^{(j)}_{k+1}) = |\nabla \mathbf{I}(\tilde{\mathbf{x}}^{(j)}_{k})|^2 \exp\left(-\frac{(d_{k+1} - d_m)^2}{2\sigma_e^2}\right) \Big/ |\nabla \mathbf{I}(\tilde{\mathbf{x}}^{(j)})| ; \quad p^{GPR}_{on}(\tilde{\mathbf{x}}^{(j)}_{k+1}) = \sqrt{|\nabla \mathbf{I}(\tilde{\mathbf{x}}^{(j)}_{k+1})|}$$

$$p_{off}(\tilde{\mathbf{x}}^{(j)}_{k+1}) = \exp\left(-\frac{|\nabla \mathbf{I}(\tilde{\mathbf{x}}^{(j)}_{k+1})|}{\mu}\right); \quad \ell(\tilde{\mathbf{x}}^{(j)}_{k+1}) = p_{on}(\tilde{\mathbf{x}}^{(j)}_{k+1}) / p_{off}(\tilde{\mathbf{x}}^{(j)}_{k+1}); \quad w^{(j)}_{k+1} = w^{(j)}_{k}\ell(\mathbf{y}(\tilde{\mathbf{x}}^{(j)}_{k+1})),$$

where $\tilde{\mathbf{x}}^{(j)}_{k+1} = (\tilde{x}^{(j)}, \tilde{y}^{(j)}, \tilde{d}^{(j)}, \tilde{\theta}^{(j)})^T = (x_{k+1}, y_{k+1}, d_{k+1}, \theta_{k+1})^T$, $j = 1,\ldots,N$, $\mathbf{r}_m = (d_m, \theta_{k+1})^T$ and σ_e is a design parameter.

The updated by the likelihood ratio $\ell(\tilde{\mathbf{x}}^{(j)}_{k+1})$ particle weights $w^{(j)}_{k+1}$, $j = 1,\ldots,N$ take part in the calculation of the updated contour estimate $\hat{\mathbf{x}}_{0:k+1} = \sum_{j=1}^{N} w^{(j)}_{k+1}\tilde{\mathbf{x}}^{(j)}_{0:k+1}$.

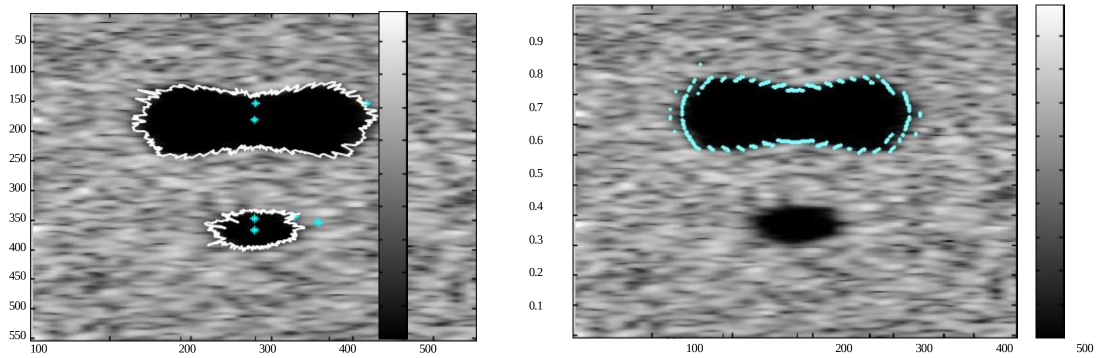

Fig.2. a) The extracted contours and magnitude

b) The points in the gate with a maximum edge

Fig.3. a) A horizontal slice of a C-scan, acquired at 1.39 nsec after the GPR signal emission [7];

b) Delineated contour of a mine target

3. Conclusion

A multiple model PF for contour determination in ultrasound medical and GPR images is designed and implemented. The filter performance is studied on a number of simulated ultrasound medical images, obtained by the simulation program Field II. It is also tested on the GPR images, published in the specialised literature. The proposed filter has shown encouraging results in terms of convergence and accuracy, achieved at the cost of acceptable computational complexity. It offers an alternative solution to this important and difficult problem.

Acknowledgements. This work is partially supported by the Bulgarian Science Funds (MI- 1506/2005), Center of Excellence BIS21++016639 and the Innovation Fund (IF-02-85/2005).

References

[1] P. Pérez, A. Blake, M. Gangnet, Jetstream: Probabilistic contour extraction with particles, Proc. Int. Conf. on Computer Vision (ICCV), II (5):524–531, (2001).
[2] P. Abolmaesumi, M. Sirouspour, An IMM PDA Filter for Cavity Boundary Extraction from Ultrasound Images, IEEE Trans. on Medical Imaging, vol.23, No 6, June (2004), 772-784.
[3] A. Doucet, N. de Freitas, N. Gordon, Eds., Sequential Monte Carlo Methods in Practice, Springer-Verlag, New York, USA, (2001)
[4] J. Jensen, Field II Ultrasound Simulation Program, Technical University of Denmark, http://www.es.oersted.dtu.dk/staff/jaj/field/ (visited 10.04.2006)
[5] P.Konstantinova, D. Adam, D. Angelova, V. Behar, Contour Determination in Ultrasound Medical Images Using IMM PDA Filter, LNCS 4310, Springer-Verlag, (2007), pp. 628–636.
[6] L. Doukovska, Hough Detector with Binary Integration Signal Processor, Comptes rendus de l'Academie bulgare des Sciences, Vol. 60, No.5, (2007), pp. 527-534.
[7] C. Lee, Mine Detection Techniques Using Multiple Sensors, ECE 501 Project, Electrical and Computer Engineering, The University of Tennessee at Knoxville. http://imaging.utk.edu/publications/papers/dissertation/cplee_project.pdf.